

Standing wave detection and interferometer application using a photodiode thinner than optical wavelength

著者	羽根 一博
journal or publication title	Applied Physics Letters
volume	75
number	14
page range	2008-2010
year	1999
URL	http://hdl.handle.net/10097/35124

doi: 10.1063/1.124898

Standing wave detection and interferometer application using a photodiode thinner than optical wavelength

Minoru Sasaki,^{a)} Xiaoyu Mi, and Kazuhiro Hane

Department of Mechatronics and Precision Engineering, Tohoku University, Sendai 980-8579, Japan

(Received 29 December 1998; accepted for publication 4 August 1999)

A thin film photodiode whose active layer is thinner than the wavelength of the incident light is described. A part of the incident photon is detected and the rest transmits through the thin film photodiode without absorption. Being inserted in the optical field, this sensor is applied to construct the new interferometer detecting the intensity profile of the standing wave of the thinnest interference fringe. © 1999 American Institute of Physics. [S0003-6951(99)03740-7]

Laser interferometry is a well-developed technique for the displacement measurement since it has high resolution and gives noncontact measuring methods.¹ In many systems (e.g., Michelson interferometer), the cubic beam splitter or the half mirror are used for making sensing and reference beams from a laser beam and for superposing these beams which have propagated each interferometer arm. The interfering beams are almost in the same propagating directions. There are some cases where the parallel interfering beams are extracted from the beams having different propagating directions using birefringent calcite prisms² or gratings.³ The obtained interference fringe is in the transverse direction. This fringe is projected onto a photodetector and the lateral shift of the fringe is measured. Another method for superposing optical beams is the optical feedback technique.⁴ The basis is the mixing between the backscattered sensing beam by the moving sample and the optical field inside the laser diode. The output intensity of the laser diode is periodically modulated with the distance of an external reflector. The advantage of this technique is the simple configuration using the laser diode as an optical phase detector as well as the light source. The disadvantages are limitation in the dynamic range of the measurement by the mode hopping of the laser diode and the lack of a stable operation.

In this study, the new interferometer based on the standing wave detection is developed. The beam splitting is not necessary and the simple configuration is realized. The laser beam is normally incident on the moving mirror and backreflected producing the standing wave. This thinnest interference fringe is measured by the photodiode whose active layer is thinner than the pitch of the standing wave.

Figure 1 shows the principle of the standing wave detection. The active layer which absorbs the photon is thinner than the wavelength of the incident light including the refractive index. The light beam transmits through the thin film photodiode before the absorption and then reflects on the downstream mirror placed on the moving sample. The reflected light beam is again incident on the active layer from the back surface. The incoming and reflected beams superpose each other. The standing wave occurs including the photodiode active layer. The conventional bulk photodiode

destroys the optical field by absorbing all of the incident light beam, whereas the thin film photodiode does not disturb the optical field very much allowing the light beam to transmit through the sensor.

The following estimation is a zeroth order approximation neglecting the absorption decay of the light intensity in the thin Si layer. E_1 is the normally incident forward propagating light beam. E_2 is the normally incident backward propagating light beam, which has reflected at the sample surface. These fields inside the active layer can be written as follows:

$$E_1 = E_0 e^{i(\omega t - kn_2 x)}, \quad (1)$$

$$E_2 = E_0 e^{i(\omega t - 2kn_1 l - 2kn_2 t_a + kn_2 x + \pi)}. \quad (2)$$

Suppose the positive direction of x points at the reflecting mirror. The region $0 \leq x \leq t_a$ is the active layer of the thin Si film, l is the distance between the active layer and the reflecting mirror. $k = 2\pi/\lambda$, λ is the wavelength of the incident light beam, and n_1 and n_2 are refractive indexes of the air and Si, respectively. The phase shift caused by the reflection and the amplitude reflectance are supposed to be π and unity, respectively. The photodiode signal I is considered to be proportional to the field intensity of the standing wave stored inside the active layer

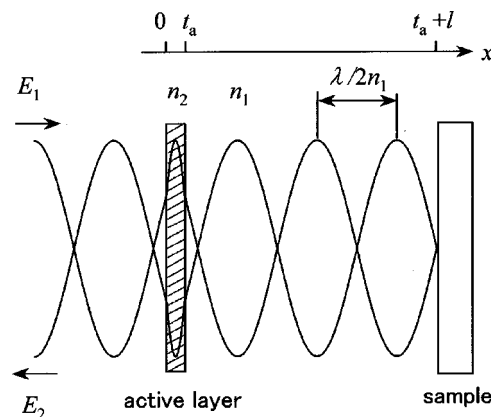


FIG. 1. Schematic diagram to explain the principle of the standing wave detection.

^{a)}Electronic mail: sasaki@hane.mech.tohoku.ac.jp

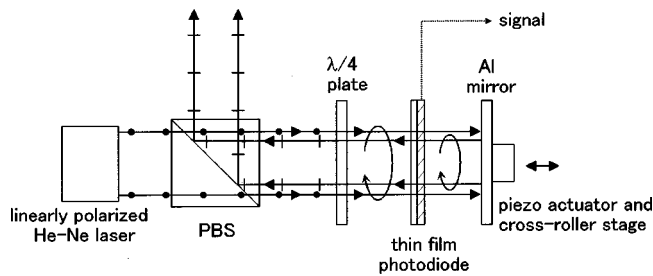


FIG. 2. Schematic diagram of the interferometer using the thin film photodiode. The polarizing beam splitter (PBS) and $\lambda/4$ plate work as an isolator. These elements are not necessary for the essence of the standing wave detection.

$$I \propto \int_0^{t_a} |E_1 + E_2|^2 dx \quad (3)$$

$$= 2E_0^2 \left\{ t_a - \frac{\sin(kn_2 t_a) \cos(2kn_1 l + kn_2 t_a)}{kn_2} \right\}. \quad (4)$$

The first term of Eq. (4) is the absorption in proportion to the film thickness. The second term is the interference signal. If the sample moves (l changes), the photodiode signal I changes having the period of $\lambda/2n_1$. When the active layer is at nodes (or antinodes) of the standing wave, the photocurrent decreases (or increases). The amplitude of the interference signal becomes maximum when the condition of $|\sin(kn_2 t_a)| = 1$ is satisfied. This condition gives the thickness of the active layer; $t_a = \lambda/4n_2 + m\lambda/2n_2$ ($m = 0, 1, 2, \dots$). Since our approximation neglects the absorption in the Si layer, the larger value of m ($= 1, 2, 3, \dots$) will be not so appropriate. Considering the refractive index of Si of ~ 3.5 , the film thickness is aimed to be 40 nm in this study. Such thin Si film will be fully depleted in the depth direction.⁵ So, the pn junction is designed to grow in the lateral direction along the sensor surface. As can be seen from Eq. (4), the contrast of the photocurrent signal can be expressed as follows:

$$\frac{I_{\max} - I_{\min}}{I_{\max} + I_{\min}} = \frac{|\sin(kn_2 t_a)|}{kn_2 t_a}. \quad (5)$$

The thinner active layer gives higher contrast up to 100%.

Figure 2 shows the schematic diagram of the interferometer. There is no reference mirror. The wave front of the incoming laser beam is the reference. The interferometer is realized using the counterpropagating two beams. The light sources are a red (632.8 nm, 7 mW) and green (543.5 nm, 0.75 mW) He-Ne laser. The reflecting mirror is placed ~ 45 mm away from the thin film photodiode, and moved by the piezo actuator.

Figure 3 shows the fabricated thin film photodiode. The initial Si-on-insulator wafer is made by the direct wafer bonding between Si and quartz. The photodiode area is 1×1 mm², and the laser beam having 1 mm diameter can be used. The overall transmission rate reaches 70% in power. Two comb shaped regions (p^+ or n^+ regions) are seen to be a slightly different color. The depletion region extends like a snake between these regions for gathering the produced photocarrier as much as possible. The apparent sensitivity of the thin film photodiode is ~ 0.01 mA/W. This value is 4 orders smaller than that of the bulk Si photodiode. This is reasonable for the present design. The absorption rate is

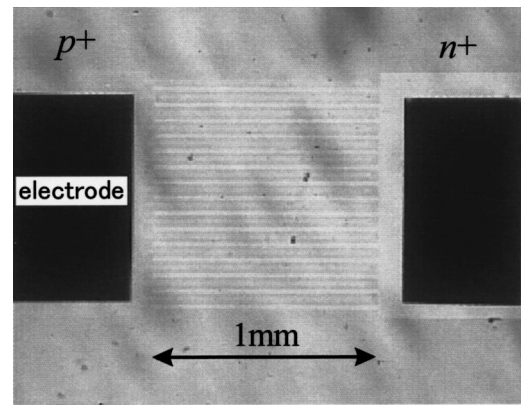


FIG. 3. Micrograph of the thin film photodiode. Thin Si film seems yellow to the human eye.

estimated to be 0.6% in power.⁶ (The transmission rate is almost decided by the reflection at Si-SiO₂ and SiO₂-air interfaces.) In addition, the high sensitivity area is 40% of the total of the photodiode area at maximum.

Figure 4 is the obtained interference signal. An interference signal having >100 nA peak-to-peak amplitude and high contrast of $\sim 80\%$ is obtained. The period is in good agreement with $\lambda/2$ for each wavelength. The new interferometer is stable and does not show any problems indicated in the optical feedback technique. The interference signal is very sensitive to the photodiode fixation and the dust adsorbed on the reflecting mirror or the photodiode surface. The interference signal is not purely sinusoidal. The signals due to the multiple-beam interference caused by the reflection at interfaces in the thin film photodiode may be included. If the reflection at interfaces is reduced using the antireflection coat or structure in the sensor, the purer standing wave profile will be obtained. The major signal still seems to be caused by the standing wave, since the overall transmission rate is 70%. The high contrast of $\sim 80\%$ cannot be explained without the signal caused by the standing wave.

Figure 5 is the relation between the signal contrast and the angle of incidence on the photodiode surface. The high contrast is obtained only in a narrow region. If the photodiode surface slants against the wave front of the incident laser beam, the interference signal having the different phase will

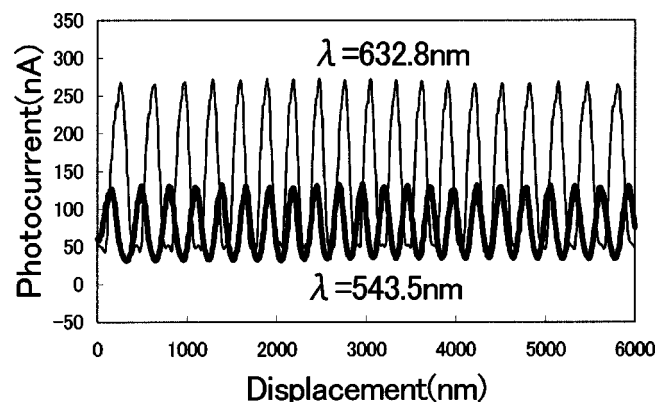


FIG. 4. The interference signal obtained from the thin film photodiode. The interference period to the lateral axis is slightly changed due to the hysteresis of the piezo actuator. Even after the mirror is moved by 20 mm using the cross-roller stage, the interference signal shows a similar amplitude and contrast.

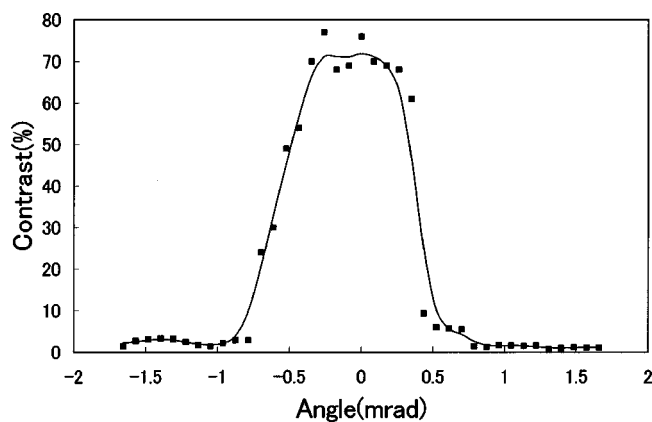


FIG. 5. . The relation between the contrast of the interference signal and the angle of incidence on the sensor surface. The light source is a red He-Ne laser.

be averaged over the detection area. The allowable angle region can be roughly estimated by $\pm \lambda/2s = \pm 0.3$ mrad (s is the span of the photodiode area: 1 mm). This value is in good agreement with the experiment.

In the Wiener's first experiment to show the existence of the standing wave, the intensity profile of the standing wave is observed after the development of the transparent photographic emulsion.⁷ Thin film photodiode realizes the real time measurement. The standing wave profile has been used inside many resonant cavity enhanced photonic devices.⁸ The sensitivity of the infrared detector is increased using the backreflection mirror and the absorption layer placed at the antinode of the standing wave.⁹ The light output intensity of the light-emitting diode is enhanced by placing the active area into an antinode position.¹⁰

In conclusion, the new photodiode whose active layer is thinner than the optical wavelength has been developed and the new interferometer is constructed detecting the standing wave. The transparency of the sensor enables us to detect a

part of the optical intensity not disturbing the optical field very much. The thin film photodiode has the high spatial resolution in its thickness direction and allows us to use the counterpropagating beams as the interfering beams. This function does not conflict with the previously developed measuring techniques. For example, the direction sensitive detection is technically feasible. If two thin film photodiodes are arrayed on the sensor substrate, two interference signals can be obtained. The phase shift of one quarter of the interference period can be obtained when a glass layer is inserted to shift the relative position between one photodiode and the standing wave profile.

This work was supported by the New Energy and Industrial Technology Development Organization. A part of this work was performed at the Venture Business Laboratory of Tohoku University.

¹ See, for example, K. J. Gäsvisk, *Optical Metrology* (Wiley, West Sussex, England); P. Hariharan, *Optical Interferometry* (Academic, N. S. W., Australia).

² D. Anselmetti, Ch. Gerber, B. Michel, H.-J. Güntherodt, and H. Rohrer, *Rev. Sci. Instrum.* **63**, 3003 (1992); J. T. Fanton and G. S. Kino, *Appl. Phys. Lett.* **51**, 66 (1987).

³ A. Kozłowska, M. Kujawińska, and C. Gorecki, *Appl. Opt.* **36**, 8116 (1997); S. Watanabe, K. Hane, and T. Goto, *Rev. Sci. Instrum.* **63**, 3856 (1992).

⁴ S. Merlo and S. Donati, *IEEE J. Quantum Electron.* **33**, 527 (1997); J. A. Smith, U. W. Rathe, and C. P. Burger, *Opt. Eng. (Bellingham)* **34**, 2802 (1995); J. Kato, N. Kikuchi, I. Yamaguchi, and S. Ozono, *Meas. Sci. Technol.* **6**, 45 (1995).

⁵ H. I. Liu, J. A. Burns, C. L. Keast, and P. W. Wyatt, *IEEE Trans. Electron Devices* **45**, 1099 (1998).

⁶ S. M. Sze, *Physics of Semiconductor Devices* (Wiley, New York).

⁷ O. Wiener, *Ann. Phys. (Leipzig)* **40**, 203 (1890).

⁸ M. S. Ünlü and S. Strite, *J. Appl. Phys.* **78**, 607 (1995).

⁹ B. Temelkuran, E. Ozbay, J. P. Kavanaugh, G. Tuttle, and K. M. Ho, *Appl. Phys. Lett.* **72**, 2376 (1998); H. Elabd and W. F. Kosonocky, *RCA Rev.* **43**, 542 (1982).

¹⁰ E. F. Schubert, Y.-H. Wang, A. Y. Cho, L.-W. Tu, and G. J. Zyzdik, *Appl. Phys. Lett.* **60**, 921 (1992).